Inorg. Chem. **2007**, *46*, 5292–5301

Characterization and Electrochemical Properties of Molecular Icosanuclear and Bidimensional Hexanuclear Cu(II) Azido Polyoxometalates

Céline Pichon,[†] Pierre Mialane,*[,†] Anne Dolbecq,[†] Jérôme Marrot,[†] Eric Rivière,[‡] Bineta Keita,[§] Louis Nadjo,*[,§] and Francis Sécheresse[†]

Institut Lavoisier, UMR 8180, Université de Versailles Saint-Quentin, 45 Avenue des Etats-Unis, 78035 Versailles Cedex, France, Institut de Chimie Moléculaire et des Matériaux d'Orsay, UMR 8182, Equipe Chimie Inorganique, Université Paris-Sud, 91405 Orsay, France, and Laboratoire de Chimie Physique, UMR CNRS 8000, Equipe d'Electrochimie et Photoélectrochimie, Université Paris 11, Bâtiment 350, 91405 Orsay Cedex, France

Received February 16, 2007

Two new Cu(II) azido polyoxometalates compounds have been synthesized, and their structures were determined by X-ray crystallography. The compound $Na_{14}[SiW_9O_{34}Cu_3(N_3)_2(OH)(H_2O)]_2 \cdot 24H_2O$ (**1**) is built from two $[SiW_9O_{34}Cu_3(\mu_{1,1,3}\text{-}N_3)_2(\mu\text{-}OH)(H_2O)]^{7-}$ subunits where the copper centers, connected by two azido ligands and one hydroxo group, form a nearly equilateral triangle. The two subunits are related by an inversion center and connected via the two $\mu_{1,1,3}$-N_3 ligands in an end-to-end fashion, affording a hexanuclear Cu(II) cluster. Linkage of these fragments via Cu—O═W bonds leads to a bidimensional arrangement of the polyoxometalate units. The complex $LiK_{14}Na_9[P_8W_{48}O_{184}Cu_{20}(N_3)_6(OH)_{18}] \cdot 60H_2O$ (**2**) consists of two $\{Cu_5(OH)_4\}^{6+}$ and two $\{Cu_5(OH)_2(\mu_{1,1,3,3}\text{-}N_3)\}^{7+}$ subunits connected via four μ-OH and four $\mu_{1,1}$-N_3 additional ligands, the 20 copper centers being encapsulated in the $[P_8W_{48}O_{184}]^{40-}$ crown polyoxotungstate ligand. **1** represents the first multidimensional compound based on azido polyoxometalate (POM) units, and **2** represents by far the largest azido POM complex isolated to date. Magnetic measurements revealed an overall antiferromagnetic behavior for both compounds. Nevertheless, the study of the variation of the magnetization with the applied field indicates that **1** possesses a triplet ground state, which can be attributed to weak ferromagnetic interaction between the $S = {}^1/_2$ triangular subunits. The stability of **1** and **2** evidenced by UV–vis spectroscopy and gel filtration chromatography, in particular at pH 5, has allowed a detailed study of their redox and electrocatalytic properties. For both compounds, the stability of the Cu(II)/Cu(I) couple is remarkable compared with the observations made in other Cu(II)-substituted POMs. Electrochemical quartz crystal microbalance measurements clearly demonstrate that the formation of the Cu(I) species occurs neatly without the formation of Cu(0). The accumulation of such Cu(II) centers within the complexes is a favorable condition to envision applications involving several electrons. The electrocatalytic reduction of dioxygen and hydrogen peroxide was achieved efficiently and has shown that the reactivity increases with the nuclearity and/or the Cu/W ratio of the POM complex. The dioxygen reduction is an overall four-electron process with water as the final product. Finally, the reduction of the W centers triggers a strong electrocatalysis of solvent reduction.

Introduction

The last two decades have witnessed an explosive growth in the synthesis and characterization of high-nuclearity magnetic clusters made of transition metals of the first row, mainly due to their relevance to molecular magnetism and bioinorganic chemistry. More generally, it is obvious that the accumulation of transition-metal centers in a single molecular unit can play a crucial role in the physical properties of inorganic molecular compounds, such as catalytic or electrocatalytic activity. Considering polyoxo-

* To whom correspondence should be addressed. E-mail: mialane@chimie.uvsq.fr (P.M.), nadjo@lcp.u-psud.fr (L.N.).
[†] Université de Versailles Saint-Quentin.
[‡] Université Paris-Sud.
[§] Université Paris 11.

10.1021/ic070313w CCC: $37.00
Published on Web 05/19/2007

metalate (POM) compounds,[1] if we exclude polyoxovanadate chemistry,[2] it is only recently that clusters with more than 10 3d metal centers have been reported. Indeed, the tetradecanuclear Cu(II) complex characterized in 2003 was the first member of this family,[3] while a spectacular complex containing up to 27 Fe(III) centers was obtained in 2005.[4] These two compounds consist in a magnetic core encapsulated by four trivacant $\{SiW_9O_{34}\}$ or four hexavacant $\{P_2W_{12}O_{48}\}$ units, respectively. Mal and Kortz have also shown that the large crown POM ligand $[H_7P_8W_{48}O_{184}]^{33-}$ can accommodate 20 Cu(II) centers connected by hydroxo groups and encapsulating a chloride anion.[5] Since 2003, our group has explored the synthesis of POMs containing azido ligands, which can act as connectors between the 3d centers embedded in a POM unit but also as intermolecular linkers between POM subunits, then leading to high-nuclearity POM complexes.[6] All the related compounds previously characterized have been obtained starting from the $[A\text{-}\alpha\text{-}PW_9O_{34}]^{9-}$, $[A\text{-}\alpha\text{-}SiW_9O_{34}]^{10-}$ or $[\gamma\text{-}SiW_{10}O_{36}]^{8-}$ POM ligands and are molecular species, with nuclearities[7] ranging from 2 to 9. The use of the trilacunary phosphononatungstate ligand in the presence of Ni(II) ions led to the dinuclear complex $[(\alpha\text{-}PW_{10}O_{37})(Ni(H_2O))_2(\mu_{1,1}\text{-}N_3)]^{6-}$, with the $[A\text{-}\alpha\text{-}PW_9O_{34}]^{9-}$ anion evolving to the $[\alpha\text{-}PW_{10}O_{37}]^{9-}$ divacant ligand during the synthesis.[8] Considering the $[\gamma\text{-}SiW_{10}O_{36}]^{8-}$ POM, two cases appeared. Retention of the dilacunary anion led to Cu(II) dinuclear and tetranuclear species, respectively.[9] On the other hand, in situ formation of the tetralacunary $[\gamma\text{-}SiW_8O_{31}]^{10-}$ anion from the $[\gamma\text{-}SiW_{10}O_{36}]^{8-}$ unit allowed the formation of the $[\{(\gamma\text{-}SiW_8O_{31})Cu_3(\mu_3\text{-}OH)(H_2O)_2(N_3)\}_3(\mu_{1,1,1,3,3,3}\text{-}N_3)]^{19-}$ nonanuclear complex.[9a] The tetranuclear compound $[(A\text{-}\alpha\text{-}SiW_9O_{34})Co_4(OH)(\mu_{1,1,1}\text{-}N_3)_2(CH_3COO)_3]^{8-}$, obtained starting from the $[A\text{-}\alpha\text{-}SiW_9O_{34}]^{10-}$ ligand, must be distinguished from the azido POM species mentioned above. Indeed, it contains both azido and acetato ligands, these last groups acting as blocking groups and preventing the formation via azido bridges of a polymeric complex.[10] Not surprisingly, the general tendency observed is that the nuclearity of the synthesized complexes increases with the number of vacancies of the POM ligand. The synthesis of high-nuclearity azido POMs must then be achieved in synthetic conditions where (i) a hydrolysis of the starting POM ligand occurs (as observed for the formation of the nonanuclear Cu(II) compound mentioned above) or (ii) the preformed multilacunary POM ligand is stable (as observed for the formation of the $[(A\text{-}\alpha\text{-}SiW_9O_{34})Co_4(OH)(\mu_{1,1,1}\text{-}N_3)_2(CH_3COO)_3]^{8-}$ complex). Focusing on the second route, we have considered the $[A\text{-}\alpha\text{-}SiW_9O_{34}]^{10-}$ and $[H_7P_8W_{48}O_{184}]^{33-}$ ligands, which are both stable in aqueous solution in reasonable temperature and pH ranges, and studied their interaction with Cu(II) and azide. We then present here the synthesis and the characterization of the hexanuclear Cu(II) compound $Na_{14}[SiW_9O_{34}Cu_3(N_3)_2(OH)(H_2O)]_2\cdot 24H_2O$ (**1**) and of the icosanuclear Cu(II) complex $LiK_{14}Na_9[P_8W_{48}O_{184}Cu_{20}(N_3)_6(OH)_{18}]\cdot 60H_2O$ (**2**). **1** represents the first multidimensional compound based on azido POM units, and **2** represents by far the largest azido POM complex isolated to date. Both compounds have been found to be stable in aqueous solution at pH 5, allowing a detailed investigation of their redox and electrocatalytic properties. Noticeably, the electrocatalytic reduction of dioxygen and hydrogen peroxide has been achieved efficiently and highlights the beneficial effect of accumulation of 3d transition-metal centers in the POM matrix.

Experimental Section

Synthesis. All chemicals were of reagent grade and were used as received. $K_{28}Li_5[H_7P_8W_{48}O_{184}]\cdot 92H_2O$[11] and $Na_{10}[A\text{-}\alpha\text{-}SiW_9O_{34}]\cdot 23H_2O$[12] have been synthesized as previously described.

$Na_{14}[SiW_9O_{34}Cu_3(N_3)_2(OH)(H_2O)]_2\cdot 24H_2O$ (1). $Na_{10}[A\text{-}\alpha\text{-}SiW_9O_{34}]\cdot 23H_2O$ (1 g, 0.348 mmol) and $Cu(CH_3COO)_2$ (194 mg, 1.068 mmol) are mixed in 6 mL of water. Then, NaN_3 (140 mg, 2.140 mmol) dissolved in 2 mL of water is added. The dark green solution is heated to 80 °C for 30 min and then cooled to room temperature. After one night, the solution is centrifugated and left in a crystallizing dish at 3 °C. A few hours later, yellow parallelepipedic crystals were collected by filtration through a glass frit and dried with ethanol and ether. Yield: 365 mg (35%). Anal. Calcd (found) for **1** ($Si_2W_{18}Cu_6H_{54}N_{12}O_{96}Na_{14}$): W 56.79 (59.74); Cu 6.54 (5.91); Na 5.52 (5.13); H 0.93 (0.92); N 2.88 (3.18). IR (cm^{-1}, KBr disk): 2103 (sh), 2079 (s), 1617 (m), 1284 (w), 999 (s), 938 (s), 907 (s), 788 (m), 746 (m), 667 (w), 527 (m). UV−vis (H_2O, 20 °C) (λ in nm (ϵ in $mol^{-1}\cdot L\cdot cm^{-1}$)): 750 (135), 880 (sh, 130).

$LiK_{14}Na_9[P_8W_{48}O_{184}Cu_{20}(N_3)_6(OH)_{18}]\cdot 60H_2O$ (2). $K_{28}Li_5[H_7P_8W_{48}O_{184}]\cdot 92H_2O$ (370 mg, 0.025 mmol), $Cu(CH_3COO)_2$ (92 mg, 0.500 mmol), and NaN_3 (120 mg, 2 mmol) are mixed in 20 mL of water. After heating to 80 °C for 15 min, an olive green solution is obtained. The solution is cooled to room temperature and left in a closed crystallizing dish. After one night, green hexagonal crystals are collected by filtration through a glass frit and washed with a minimum amount of 2 M KCL, ethanol, and ether. Yield: 200 mg (50%). Anal. Calcd (found) for **2** ($P_8W_{48}Cu_{20}H_{138}N_{18}O_{262}LiK_{14}Na_9$): W 56.25 (56.16); Cu 8.10 (7.15); K

(1) (a) Pope, M. T. *Heteropoly and Isopoly Oxometalates*; Springer-Verlag, Berlin, 1983. (b) Hervé, G.; Tézé, A.; Contant, R. In *Polyoxometalate Molecular Science*; Borrás-Almenar, J. J., Coronado, E., Müller, A., Pope, M. T., Eds.; Kluwer Academic Publishers: Dordrecht, The Netherlands, 2003. (c) *Polyoxometalate Chemistry for Nano-composite Design*; Yamase, T., Pope, M. T., Eds.; Kluwer Academic Publishers: Dordrecht, The Netherlands, 2002. (d) Hill, C. L., Ed. Polyoxometalates. *Chem. Rev.* **1998**, *98*, 1−390. (e) Contant, R.; Hervé, G. *Rev. Inorg. Chem.* **2002**, *22*, 63. (f) Long, D.-L.; Burkholder, E.; Cronin, L. *Chem. Soc. Rev.* **2007**, *36*, 105.

(2) (a) Khan, M. I.; Zubieta, J. *Prog. Inorg. Chem.* **1995**, *43*, 1. (b) Chen, Q.; Zubieta, J. *Coord. Chem. Rev.* **1992**, *114*, 107.

(3) Mialane, P.; Dolbecq, A.; Marrot, J.; Rivière, E.; Sécheresse, F. *Angew. Chem., Int. Ed.* **2003**, *42*, 3523.

(4) Godin, B.; Chen, Y.-G.; Vaissermann, J.; Ruhlmann, L.; Verdaguer, M.; Gouzerh, P. *Angew. Chem., Int. Ed.* **2005**, *44*, 3072.

(5) Mal, S. S.; Kortz, U. *Angew. Chem., Int. Ed.* **2005**, *44*, 3777.

(6) Mialane, P.; Dolbecq, A.; Sécheresse, F. *Chem. Commun.* **2006**, 3477.

(7) Throughout the text, the term nuclearity refers to the number of neighboring paramagnetic centers.

(8) Mialane, P.; Dolbecq, A.; Rivière, E.; Marrot, J.; Sécheresse, F. *Angew. Chem., Int. Ed.* **2004**, *43*, 2274.

(9) (a) Mialane, P.; Dolbecq, A.; Marrot, J.; Rivière, E.; Sécheresse, F. *Chem.—Eur. J.* **2005**, *11*, 1771. (b) Mialane, P.; Duboc, C.; Marrot, J.; Rivière, E.; Dolbecq, A.; Sécheresse, F. *Chem.—Eur. J.* **2006**, *12*, 1950.

(10) Lisnard, L.; Mialane, P.; Dolbecq, A.; Marrot, J.; Clemente-Juan, J. M.; Coronado, E.; Keita, B.; de Oliveira, P.; Nadjo, L.; Sécheresse, F. *Chem.—Eur. J.* **2007**, *13*, 3525.

(11) Contant, R.; Tézé, A. *Inorg. Chem.* **1985**, *24*, 4610.

(12) Tézé, A.; Hervé, G. *Inorg. Synth.* **1990**, *27*, 85.

Table 1. Crystallographic Data for **1** and **2**

	1	**2**
empirical formula	$Si_2W_{18}Cu_6H_{54}N_{12}O_{96}Na_{14}$	$P_8W_{48}Cu_{20}H_{138}N_{18}O_{262}LiK_{14}Na_9$
fw (g)	5826.9	15 687.4
T (K)	100	293
cryst syst	monoclinic	tetragonal
space group	$P2(1)/c$ (No. 14)	$I4/m$ (No. 87)
a (Å)	13.1745(9)	25.7938(3)
b (Å)	18.5992(12)	25.7398(3)
c (Å)	22.5851(13)	22.0081(5)
β (deg)	92.244(3)	90
V (Å^3)	5529.9(6)	14642.4(4)
Z	2	2
d_{calc} (g cm^{-3})	3.553	3.412
cryst size (mm)	0.18 × 0.14 × 0.12	0.24 × 0.20 × 0.18
reflns collected/unique	71118/9740 (R_{int} = 0.0489)	177005/10976 (R_{int} = 0.0474)
GOF	1.230	1.274
R (>2σ(I))	$R_1(F_o)^a$ = 0.0418 $R_2(F_o^2)^b$ = 0.1203	$R_1(F_o)^a$ = 0.0413 $R_2(F_o^2)^b$ = 0.1191
R (all data)	$R_1(F_o)^a$ = 0.0484 $R_2(F_o^2)^b$ = 0.1372	$R_1(F_o)^a$ = 0.0663 $R_2(F_o^2)^b$ = 0.1609

[a] $R_1 = (\sum|F_o| - |F_c|)/(\sum|F_c|)$. [b] $R_2 = (\sum w(F_o^2 - F_c^2)^2)/(\sum w(F_o^2)^2)^{1/2}$.

3.49 (3.47); P 1.58 (1.54); H 0.89 (0.82); N 1.61 (1.62); Na 1.32 (1.26). IR (cm^{-1}, KBr disk): 2100 (s), 2084 (s), 1617 (m), 1293 (w), 1230 (w), 1129 (s), 1084 (s), 1011 (w), 961 (s), 941 (s), 903 (s), 807 (s), 733 (s), 605 (s). UV−vis (H_2O, 20 °C) (λ in nm (ϵ in mol^{-1}·L·cm^{-1})): 745 (1150), 850 (sh, 950).

Infrared spectra were recorded on a IRFT Magna 550 Nicolet spectrophotometer using the technique of pressed KBr pellets.

X-ray Diffraction. For **1** and **2**, intensity data collection were carried out with a Brucker Nonius X8 APEX 2 diffractometer with a CCD detector using Mo Kα monochromatized radiation (λ = 0.71073 Å). For **1**, a single crystal was mounted on a glass fiber in Paratone-N oil, and intensity data were recorded at 100 K. For **2**, a single crystal was mounted in a capillary tube and recorded at 300 K. The absorption correction was based on multiple and symmetry-equivalent reflections in the data set using the *SADABS* program (Sheldrick, G. M. *SADABS, Program for Scaling and Correction of Area Detector Data*; University of Göttingen; Göttingen, Germany, 1997) based on the method of Blessing. The structure was solved by direct methods and refined by full-matrix least-squares using the *SHELX-TL* package (Sheldrick, G. M. *SHELX-TL, version 5.03, Software Package for the Crystal Structure Determination*; Siemens Analytical X-ray Instrument Division: Madison, WI, 1994). All the atoms were refined anisotropically except for some disordered alkali counterions and free water molecules. In complex **2**, disordered azido and hydroxo ligands have been refined with the site occupation factors 0.5 (see below). Crystallographic data are given in Table 1.

Magnetic Measurements. Magnetic susceptibility measurements were carried out with a Quantum Design SQUID Magnetometer with an applied field of 1000 G using powder samples pressed in pellets to avoid preferential orientation of the crystallites. The independence of the susceptibility value with regard to the applied field was checked at room temperature. The susceptibility data were corrected from the diamagnetic contributions, as deduced by using Pascal's constant tables.

Electrochemical and UV−Vis Studies. Chemicals. Pure water was used throughout. It was obtained by passing water through a RiOs 8 unit followed by a Millipore-Q Academic purification set. All the chemicals were of high-purity grade and were used as received. All reagents were used as purchased without further purification. In the present study, the pH 5 value is imposed by 1 M ($CH_3COOLi + CH_3COOH$).

Gel Filtration Chromatography. A gel filtration chromatography analysis performed in 0.4 M (CH_3COONa/CH_3COOH) (pH = 5) carried out in the same experimental conditions as previously reported[13] indicates that **1** elutes far earlier than $[P_2W_{15}Mo_2VO_{62}]^{8-}$ ($Mo_2VP_2W_{15}$) (ionic mass = 4055). This rules out the possibility of **1** breaking down into two $[SiW_9O_{34}Cu_3(N_3)_2(OH)(H_2O)]^{7-}$ trinuclear units, since the latter would have a molecular weight of 2536 and therefore would elute later, and this indicates that the hexanuclear unit is maintained in solution.

Equipment and Apparatus. UV−vis spectra were recorded on a Perkin-Elmer Lambda 19 spectrophotometer. The UV−vis spectrophotometry stability studies of **1** and **2** showed that these compounds are stable for several hours in various pH media, including the pH 5 medium exclusively used in this work. For electrochemical experiments, the solutions were deaerated thoroughly for at least 30 min with pure argon and kept under a positive pressure of this gas during the experiments. The sourcing, mounting, and polishing of the glassy-carbon (GC, Le Carbone Lorraine, France) electrodes have been described elsewhere.[14] The glassy-carbon samples had a diameter of 3 mm. The electrochemical setup was an EG&G 273 A driven by a PC with the 270 software. Potentials are quoted against a saturated calomel electrode (SCE). The counter electrode was a platinum gauze of large surface area. All experiments were performed at the laboratory temperature.

Electrochemical quartz crystal microbalance (EQCM). The EQCM setup used in this work was the system QCA 922 (Seiko/EG&G) with 9 MHz AT-cut crystals. New crystals equipped with carbon electrodes (4.5 mm diameter) were provided by Seiko and allowed working in media where classical gold or platinum electrodes were inappropriate. The data from the QCA 922 setup were first recorded in the computer and then printed.[15] Frequency variations are recorded and are the only data necessary for the discussion in this work. However, the expressions mass increase or mass decrease will also be used routinely as equivalent to frequency decrease or frequency increase, respectively.

Results and Discussion

Complexes **1** and **2** were synthesized in water (pH 5) with heating at 80 °C in the presence of an excess of NaN_3. In each case, single crystals are obtained from the filtrate. Attempts to synthesize complex **2** in analogous conditions but using $CuCl_2$ instead of $Cu(CH_3COO)_2$ led to the $[Cu_{20}Cl(OH)_{24}(H_2O)_{12}(P_8W_{48}O_{184})]^{25-}$ complex previously reported.[5] This highlights that for this last compound (i) the chloride anion acts as a template agent in the formation of the $\{Cu_{20}Cl(OH)_{24}(H_2O)_{12}\}$ cluster and (ii) the hydroxo groups connecting the Cu(II) centers in this complex cannot be substituted by azido groups.

Structure of Complex 1. Compound **1** is formed of two $[SiW_9O_{34}Cu_3(N_3)_2(OH)(H_2O)]^{7-}$ subunits (Figure 1a) related by an inversion center and connected via azido ligands, forming a hexanuclear Cu(II) unit (Figure 1b). Linkage of these $\{Cu_6\}$ fragments via Cu−O═W bonds leads to a bidimensional arrangement of the POM hexanuclear species

(13) Bassil, B. S.; Kortz, U.; Tigan, A. S.; Clemente-Juan, J. M.; Keita, B.; de Oliveira, P.; Nadjo, L. *Inorg. Chem.* **2005**, *44*, 9360.
(14) Keita, B.; Nadjo, L. *J. Electroanal. Chem.* **1988**, *243*, 87.
(15) Keita, B.; Contant, R.; Abdeljalil, E.; Girard, F.; Nadjo, L. *Electrochem. Commun.* **2000**, *2*, 295.

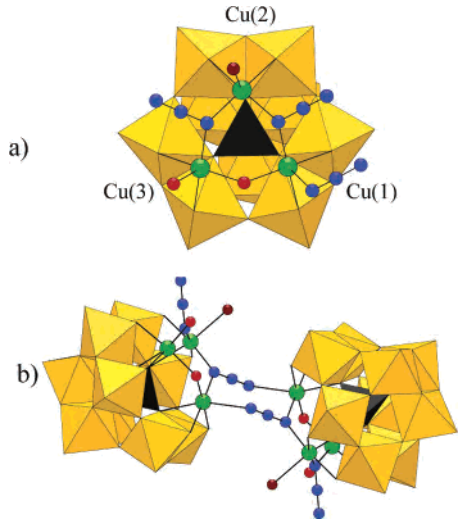

Figure 1. Polyhedral and ball-and-stick representations of (a) the trinuclear $[SiW_9O_{34}Cu_3(N_3)_2(OH)(H_2O)]^{7-}$ subunit in **1**; (b) the hexanuclear $[(SiW_9O_{34}Cu_3(N_3)_2(OH)(H_2O))_2]^{14-}$ unit in **1**. Yellow octahedra, $\{WO_6\}$; black tetrahedra, $\{SiO_4\}$; green spheres, Cu; red spheres, O; blue spheres, N; brown spheres, H_2O.

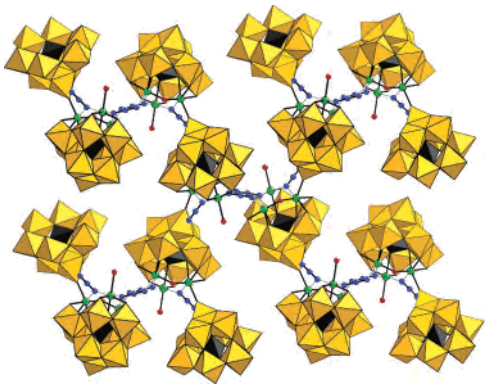

Figure 2. Polyhedral and ball-and-stick representation of compound **1** showing the 2D arrangement of the $[(SiW_9O_{34}Cu_3(N_3)_2(OH)(H_2O))_2]^{14-}$ units. Yellow octahedra, $\{WO_6\}$; black tetrahedra, $\{SiO_4\}$; green spheres, Cu; red spheres, O; blue spheres, N.

(Figure 2). Each $[SiW_9O_{34}Cu_3(N_3)_2(OH)(H_2O)]^{7-}$ subunit consists of the $[A\text{-}\alpha\text{-}SiW_9O_{34}]^{10-}$ ligand accommodating three Cu(II) centers, which form a triangular unit where the paramagnetic ions are connected via two crystallographically independent basal−basal end-on azido ligands (d_{Cu-N} = 1.995(8)−2.032(8) Å; Cu−N(N$_2$)−Cu = 126.0(4)° and 129.0(4)°) and a hydroxo bridge (d_{Cu-OH} = 1.954(8) Å and 1.973(8) Å; Cu−O(H)−Cu = 127.5(4)° and 129.0(4)°). The nature of the hydroxo bridge is confirmed by valence bond calculations (VBS = 0.93).[16] Whereas one of the azido ligand acts as a $\mu_{1,1}$ ligand, the other one acts as a $\mu_{1,1,3}$ ligand, allowing the formation of the hexanuclear unit via a long axial Cu−N bond ($d_{Cu-N(N2)}$ = 2.583(9) Å). All the copper atoms are tricoordinated to the POM ligand and reside in an axially distorted octahedral environment. The sixth position of the Cu(2) center is occupied by a terminal water molecule represented as a brown sphere in Figure 1a (d_{Cu-OH} = 2.430(13) Å, VBS = 0.13), while the Cu(3) atom is connected to

(16) Brese, N. E.; O'Keeffe, M. *Acta Crystallogr., Sect. B* **1991**, *47*, 192.

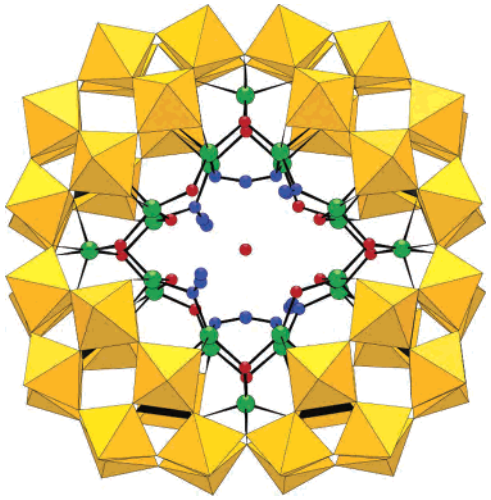

Figure 3. Polyhedral and ball-and-stick representation of the anion $[P_8W_{48}O_{184}Cu_{20}(N_3)_6(OH)_{18}]^{24-}$ in **2**. Yellow octahedra, $\{WO_6\}$; black tetrahedra, $\{PO_4\}$; green spheres, Cu; red spheres, O; blue spheres, N.

a O=W oxygen atom of an adjacent hexanuclear unit, allowing the formation of the two-dimensional (2D) structure. These Cu···O=W bonds are dramatically shorter (d_{Cu-OW} = 2.230(7) Å) than those found in polymeric Cu(II) polyoxometalates previously reported ($2.4 \lesssim d_{Cu\cdots O=W} \lesssim 2.8$ Å).[17]

Structure of Complex 2. Complex **2** crystallizes in the quadratic space group *I*4/*m*. It can be described as a cluster containing four connected pentanuclear Cu(II) subunits encapsulated by the crown polyoxotungstate ligand $[P_8W_{48}O_{184}]^{40-}$ (Figure 3). In each subunit, the five Cu(II) ions form a square pyramid, two μ_3-hydroxo ligands connecting the apical Cu(II) center to the four basal copper cations ($d_{Cu-O(H)}$ = 1.938(3)−2.070(3) Å). Such an arrangement has been previously observed in the pentanuclear cluster $[Cu_5(OH)_4(H_2O)_2(A\text{-}\alpha\text{-}SiW_9O_{33})_2]^{10-}$.[18] In each $\{Cu_5\}$ fragment constituting complex **2**, the apical copper ion is in an axially distorted environment, the four remaining paramagnetic centers being in a distorted-trigonal-bipyramidal environment. A crystallographic disorder in the $\{Cu_5\}$ fragments between the hydroxo and azido ligands connecting the Cu(II) ions has been solved, revealing that **2** contains two different $\{Cu_5\}$ subunits. In the first one, the basal plane of the $\{Cu_5\}$ square pyramid is formed of two $\{Cu(\mu\text{-}OH)Cu\}$ pairs, leading to a $\{Cu_5(OH)_4\}^{6+}$ cluster, while in the second one, a $\mu_{1,1,3,3}$ ligand connects the four Cu(II) centers, affording the $\{Cu_5(OH)_2(\mu_{1,1,3,3}\text{-}N_3)\}^{7+}$ fragment (d_{Cu}−X = 1.891(2) Å; Cu−X−Cu = 129.8(3)° and 130.1(3)° (X = N, O)). Such a coordination mode for an azido ligand remains rare[19] and has been observed in a Cu(II) cluster only very recently.[20] However, as the tetradentate ligand is connected to four equatorial positions of the Cu(II) ions in **2** and four

(17) (a) Lisnard, L.; Dolbecq, A.; Mialane, P.; Marrot, J.; Sécheresse, F. *Inorg. Chim. Acta* **2004**, *357*, 845. (b) Lisnard, L.; Dolbecq, A.; Mialane, P.; Marrot, J.; Codjovi, E.; Sécheresse, F. *Dalton Trans.* **2005**, 3913. (c) Reinoso, S.; Vitoria, P.; Gutiérrez-Zorilla, J. M.; Lezama, L.; San Felices, L.; Beitia, J. I. *Inorg. Chem.* **2005**, *44*, 9731.

(18) Hua, L.-H.; Kortz, U. *Inorg. Chem.* **2004**, *43*, 7961.

(19) (a) Meyer, F.; Kircher, P.; Pritzkow, H. *Chem. Commun.* **2003**, 774. (b) Demeshko, S.; Leibeling, G.; Marringele, W.; Meyer, F.; Mennerich, C.; Klaus, H.-H.; Pritzkow, H. *Inorg. Chem.* **2005**, *44*, 519.

(20) Nanda, P. K.; Aromí, G.; Ray, D. *Chem. Commun.* **2006**, 3181.

axial positions of the copper centers in the tetranuclear complex previously reported, the Cu−N distances are dramatically longer for this last complex. We can also note than in **2**, the $\{Cu_4(\mu_{1,1,3,3}\text{-}N_3)\}$ fragment adopts an eclipsed conformation (C_{2v} symmetry), while a staggered conformation (C_{2h} symmetry) was observed in the complex reported by Ray et al. Finally, each $\{Cu_5\}$ group is connected to two adjacent pentanuclear subunits via two disordered μ-OH and two $\mu_{1,1}$-N_3 bridging ligands (d_{Cu-X} = 1.984(4) and 1.985(4) Å; Cu−X−Cu = 117.7(2)° (X = N, O)), leading to the formation of an icosanuclear Cu(II) cluster enclosing a water molecule in its center with a shortest $(H_2)O\cdots O(H)$ distance of 3.395(5) Å.

Spectroscopic and Magnetic Characterization. The IR spectra of compounds **1** and **2** exhibit two distinct bands in the 2000−2150 cm^{-1} range assigned to the asymmetric stretching vibration of the azido ligands (ν_{as} = 2103 and 2079 cm^{-1} for **1**; ν_{as} = 2100 and 2084 cm^{-1} for **2**). This confirms the presence of two crystallographically independent N_3^- groups in these two compounds. Symmetric stretching vibrations are also observed (ν_s = 1284 cm^{-1} for **1**; ν_s = 1293 cm^{-1} for **2**). For compound **1**, the ν_s vibration can be attributed to both the $\mu_{1,1}$ and $\mu_{1,1,3}$-N_3 ligands, as the tridentate ligand coordinates the Cu(II) centers in an asymmetric fashion. In the case of compound **2**, the symmetric stretching vibration mode can be attributed only to the $\mu_{1,1}$ ligands, as the $\mu_{1,1,3,3}$ ligands bridge the paramagnetic centers in a symmetric coordination mode. Despite the presence of acetate in the synthetic media, the IR spectrum of complex **1** confirmed that in the solid-state this ligand does not bind the transition-metal centers constituting this compound, in contrast with the Co(II) complex $[(A\text{-}\alpha\text{-}SiW_9O_{34})Co_4(OH)(\mu_{1,1,1}\text{-}N_3)_2(CH_3COO)_3]^{8-}$ synthesized in analogous conditions.[10] The electronic spectra of compounds **1** and **2** in aqueous solution have been recorded (Supporting Information, parts a and b, respectively, of Figure SI1). In the visible region, each of these spectra exhibits two ligand-field bands (λ = 750 and 880 nm for **1**; λ = 745 and 850 nm for **2**), the second one observed as a shoulder. For complex **1**, these bands can be ascribed to the $d_{xy} \rightarrow d_{x^2-y^2}$ and $d_{z^2} \rightarrow d_{x^2-y^2}$ transitions, respectively, as expected for trans-distorted-octahedral Cu(II) compounds with a $d_{x^2-y^2}$ ground state.[21] An attribution of these transitions cannot be easily done in the case of compound **2**, as this complex contains both distorted-octahedral and square-pyramidal Cu(II) ions.

The magnetic behavior of the two compounds has been studied. At 300 K, the $\chi_M T$ product, χ_M being the magnetic susceptibility for one mole of compound **1**, is equal to 2.30 $cm^3\ mol^{-1}$ K, a value lower than expected for six Cu(II) centers ($\chi_M T$ = 2.48 $cm^3\ mol^{-1}$ K, assuming g = 2.1). The $\chi_M T = f(T)$ curve decreases upon sample cooling (Figure 4), reaching a $\chi_M T$ value of 1.07 $cm^3\ mol^{-1}$ K at 2 K. This behavior is characteristic of an antiferromagnetic coupling. The same behavior has been observed for complex **2** (Supporting Information, Figure SI2), the $\chi_M T = f(T)$ curve decreasing continuously from 300 K where $\chi_M T$ is equal to 5.12 $cm^3\ mol^{-1}$ K with an expected value of $\chi_M T$ = 8.27 $cm^3\ mol^{-1}$ K for 20 uncoupled Cu(II) centers (assuming g = 2.1) to 2 K ($\chi_M T$ = 1.48 $cm^3\ mol^{-1}$ K). For both compounds, it has not been possible to quantify the magnetic-exchange parameters using a Heisenberg−Dirac−Van Vleck Hamiltonian, but the overall behavior has been qualitatively rationalized.

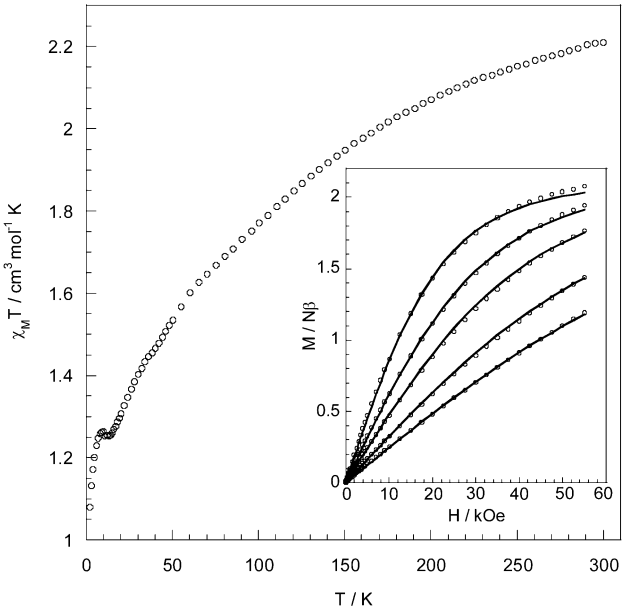

Figure 4. Thermal dependence of $\chi_M T$ for **1**. Inset: magnetization versus magnetic field at 2, 3, 4, 6 and 8 K (from top to bottom); the solid lines represent the best-fitting results (see text).

In compound **1**, the magnetic coupling must be dominated by the exchange interactions inside each $[SiW_9O_{34}Cu_3(N_3)_2(OH)(H_2O)]^{7-}$ trinuclear subunit, in which the large Cu−O(H)−Cu[22] and Cu−$N(N_2)$−Cu[23] bridging angles (θ_{av} = 127.5° and 128.25°, respectively) associated to a basal−basal end-on coordination mode of the azido ligands must impose relatively strong antiferromagnetic interactions, affording a $S = {}^1/_2$ ground state. On another hand, the formation of the Cu(II) hexanuclear unit constituting **1** is ensured by two asymmetric end-to-end azido bridges. Such a coordination mode induces magnetic coupling ranging from slightly ferromagnetic to slightly antiferromagnetic.[24] Compound **1** can then possess either a singlet or a triplet ground state. The variation of the magnetization M with the applied field H for **1** in the range of 0−5.5 T has been recorded at 2, 3, 4, 6, and 8 K (Figure 4, inset). The best fit of the $M = f(H)$ curves has been obtained considering the axial zero-field splitting Hamiltonian $\hat{H} = -D(\hat{S}_z^2 - \hat{S}(\hat{S}+1))$ with S = 1, leading to D = 1.40 cm^{-1} and g = 2.10 ($R = 1.3 \times 10^{-4}$).[25] On another hand, it has not been possible to reproduce the $M = f(H)$ curve recorded at 2 K considering two $S = {}^1/_2$ isolated centers. This suggests that the two triangular units

(21) Hathaway, B. J.; Billing, D. E. *Coord. Chem. Rev.* **1970**, *5*, 143.

(22) (a) Crawford, W. H.; Richardson, H. W.; Wasson, J. R.; Hodgson, D. J.; Hatfield, W. E. *Inorg. Chem.* **1976**, *15*, 2107. (b) Ruiz, E.; Alemany, P.; Alvarez, S.; Cano, J. *J. Am. Chem. Soc.* **1997**, *119*, 1297.

(23) Thompson, L. K.; Tandon, S. S.; Manuel, M. E. *Inorg. Chem.* **1995**, *34*, 2356.

(24) Triki, S.; Gómez-García, C. J.; Ruiz, E.; Sala-Pala, J. *Inorg. Chem.* **2005**, *44*, 5501.

(25) $R = [\sum(M_{calc} - M_{obs})^2/\sum(M_{obs})^2]$.

are ferromagnetically coupled. This result can be compared to those found for the $[Cu_2(N_3)_2(Et_3dien)_2]^{2+}$ (Et_3dien = triethyldiethylenetriamine)[26] and $[Cu_2(bben)_2(N_3)_4]_n$ (bben = 1,2-bis(benzylamino)ethane)[27] dinuclear complexes and for the monodimensional compound $[Cu(4\text{-}(dimethylamino)pyridine)(N_3)_2]_\infty$,[28] where the asymmetric end-to-end azido bridging ligands have been shown to mediate ferromagnetic-exchange interactions. We can also note that the calculated D value is higher than those previously determined in Cu(II) POMs for a triplet state ($|D| = 0.51$ and $0.96\ cm^{-1}$, respectively).[9b]

Analogously, we can try to rationalize qualitatively the magnetic behavior of complex **2**, considering first the interactions occurring in the pentanuclear Cu(II) subunits. As mentioned above, the two $\{Cu_5(OH)_4\}^{6+}$ fragments present in **2** are closely related to that found in the $[Cu_5(OH)_4(H_2O)_2(A\text{-}\alpha\text{-}SiW_9O_{33})_2]^{10-}$ POM, which exhibits an antiferromagnetic behavior.[29] The second type of fragment observed in **2**, $\{Cu_5(OH)_2(N_3)\}^{7+}$, is formally obtained by replacing two μ-OH ligands by one $\mu_{1,1,3,3}$-N_3 bridge. As the symmetric end-to-end coordination mode and end-on coordination mode with a large bridging angle ($Cu-N(N_2)-Cu = 129.8(3)°$ and $130.1(3)°$ in **2**) both induce antiferromagnetic coupling, this fragment must also possess a doublet ground state. Finally, the pentanuclear subunits are connected by μ-hydroxo and basal−basal $\mu_{1,1}$-N_3 ligands with large bridging angles ($Cu-X-Cu = 117.7(2)°$ (X = N, O)) and must then be antiferromagnetically coupled, justifying the $\chi_M T = f(T)$ behavior observed in the Supporting Information, Figure SI2.

Electrochemistry. In the Supporting Information, Figure SI3 shows the cyclic voltammogram (CV) of **1** at pH 5. The shape and large current intensity of the copper desorptive wave on the CV obscure the actual behaviors of the other waves. The CV ends, at the extreme negative potential limit, by a very large current chemically irreversible wave (not shown), which might feature plurielectronic processes of W centers and/or the electrolyte limit. On an expanded current scale, Figure 5a reveals that the CV of **1** is constituted by four waves with their reduction peaks located respectively at −0.168, −0.298, ∼−0.700, and −0.900 V. The last two waves are attributed to the reduction of W(VI) centers. The first two waves are associated, on potential reversal, with a large current intensity, an apparently unique oxidation wave peaking at +0.023 V, with the characteristic shape usually encountered in the oxidation of surface-adsorbed species. These two reduction waves are attributed to the reduction in two steps of the Cu(II) centers to Cu(0) through the Cu(I) state. This overall behavior is in agreement with the observations made with other Cu(II)-substituted POMs in

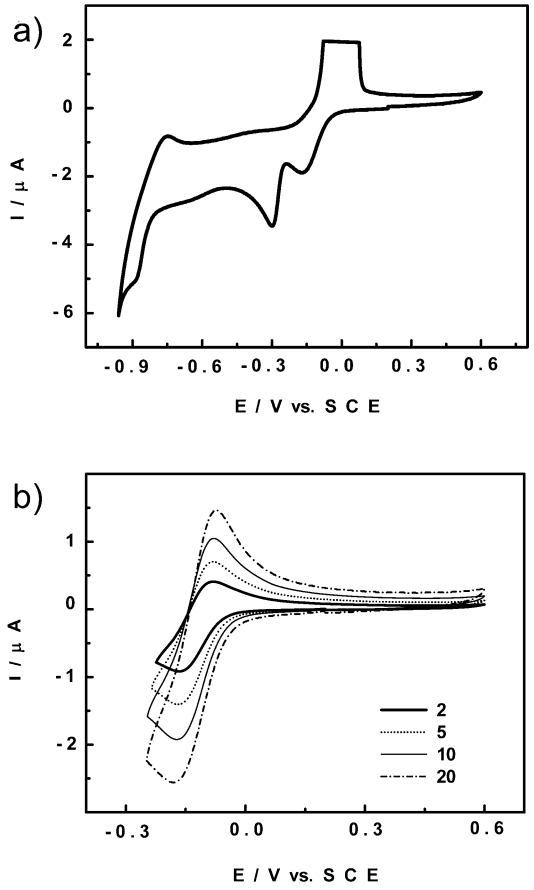

Figure 5. (a) Cyclic voltammograms of a 10^{-4} M solution of **1** in a pH 5 medium. The scan rate was 10 mV s^{-1}, and the working electrode was glassy carbon (3 mm diameter disc). A magnified scale was used to highlight the presence of a drawn-out wave. The copper reoxidation wave was truncated. (b) Cyclic voltammogram of **1** restricted to the potential domain of the Cu(II) to Cu(I) redox process. The scan rates are indicated in the cartoon. For further details, see the text.

the same experimental conditions.[29,30] The shape of these Cu(II) redox processes resembles that observed with $Cu(SO_4)$,[30b] but the resemblance is only qualitative. As a matter of fact, the presence of the ligands is mainly reflected in the ΔE values between the two cathodic peak potentials for the reduction steps of Cu(II): the ΔE values are 0.286 and 0.130 V, respectively, for $Cu(SO_4)$ and **1**. It must be concluded that, in this medium, the Cu(II) centers are not released from **1** in solution. Also, as can be anticipated, the POM ligand has little influence, if any, on the potential location of the oxidation wave of the deposited Cu(0).

Upon restriction of the potential domain to the Cu(II) to Cu(I) process, this redox couple appears to be quasi-reversible (the anodic to cathodic peak potential difference is 0.092 V), with the associated oxidation peak located at −0.076 V, which is lower compared with the value observed for the peak potential obtained for the Cu(0) to Cu(II) oxidation (+0.023 V). Figures 5b and SI4 (Supporting Information) indicate that the Cu(II)/Cu(I) electron transfer

(26) Escuer, A.; Font-Bardia, M.; Massoud, S. S.; Mautner, F. A.; Peñalba, E.; Solans, X.; Vicente, R. *New. J. Chem.* **2004**, *28*, 681.
(27) Xie, Y.; Liu, Q.; Jiang, H.; Du, C.; Xu, X.; Yu, M.; Zhu, Y. *New J. Chem.* **2002**, *26*, 176.
(28) Dalai, S.; Mukherjee, P. S.; Mallah, T.; Drew, M. G. B.; Chauduri, N. R. *Inorg. Chem. Commun.* **2002**, *5*, 472.
(29) Nellutla, S.; van Tol, J.; Dalal, N. S.; Bi, L.-H.; Kortz, U.; Keita, B.; Nadjo, L.; Khitrov, G. A.; Marshall, A. G. *Inorg. Chem.* **2005**, *44*, 9795.
(30) Representative references include: (a) Keita, B.; Mbomekalle, I. M.; Nadjo, L.; Contant, R. *Electrochem. Commun.* **2001**, *3*, 267. (b) Keita, B.; Mbomekalle, I. M.; Nadjo, L. *Electrochem. Commun.* **2003**, *5*, 830. (c) Jabbour, D.; Keita, B.; Nadjo, L.; Kortz, U.; Mal, S. S. *Electrochem. Commun.* **2005**, *7*, 841.

is essentially governed by a diffusion process. Altogether, these observations converge to explain why an apparently single large current oxidation wave corresponds to the two-step Cu(II) to Cu(0) reduction processes: (i) The two oxidation waves are only separated by roughly 0.1 V. (ii) The Cu(I)/Cu(II) diffusion wave is substantially smaller than the oxidation current of Cu(0), which features a surface-confined process.

Following CV curves, it was expected that setting the potential to −0.450 V vs SCE should permit the reduction of all Cu(II) centers to the Cu(0) state. The charge consumption turns out to be 12.10 electrons per molecule of **1**, thus indicating that all the six Cu(II) centers are effectively reduced to the Cu(0) state. During this electrolysis, the characteristic color of deposited Cu(0) was observed on the electrode surface. In addition, the solution did not turn blue, a feature that would have indicated a reduction of W centers. This characteristic blue color was effectively observed when the working electrode potential was fixed at a value more negative than −0.450 V. In this last domain, along with the reduction of W centers, catalysis of the solvent reduction was also observed, triggered by the deposited Cu(0). Comparison of the peak current intensities for the Cu(II) to Cu(I) reduction processes for **1** and for $Cu(SO_4)$ indicates that the diffusion coefficient of **1** is roughly 3.5 times smaller than that for $Cu(SO_4)$, thus demonstrating that Cu(II) cations are not free in solution.

In summary, the POM ligands of **1** have permitted an accumulation of six Cu(II) centers to build up a complex that remains stable in the pH 5 medium. In addition, the CVs of this complex show that the ligands also stabilize the Cu(I) form within the complex. It is worth noting that the reversibility of the present Cu(II)/Cu(I) system is substantially improved when compared with the same system in other sandwich-type POMs like $[Cu_4(H_2O)_2(P_2W_{15}O_{56})_2]^{16-}$.[30b] The behavior of this Cu(II)/Cu(I) couple permits one to envision a clear evaluation of electrocatalytic applications in which the Cu(I) form is considered to be the effectively active species. Finally, it was necessary to solve the following issue: the stability of the Cu(I) form in the present experimental conditions and in the voltammetric time scale should be cross-checked to ascertain that tiny amounts of Cu(0) deposit, undetectable by CV, are not occurring as a result of a disproportionation process or an underpotential deposition process. An EQCM was used for this purpose.

For an easy comparison with the previous CV experiments, the working EQCM electrode was a crystal covered with a carbon film. Figure 6a shows the CV corresponding to the reduction of the Cu(II) centers of **1** at pH 5 on this carbon film. Obviously the observed wave shape is the same as that previously obtained on a glassy-carbon surface, which is a strong indication of the good quality of the carbon film of the EQCM. The CV obtained in the electrolyte alone is also superimposed in Figure 6a and shows that there is no appreciable electroactive process in the absence of **1**. Figure 6b shows the EQCM frequency response recorded simultaneously with the CV pattern of Figure 6a. Several domains can be distinguished. During the forward potential scan from

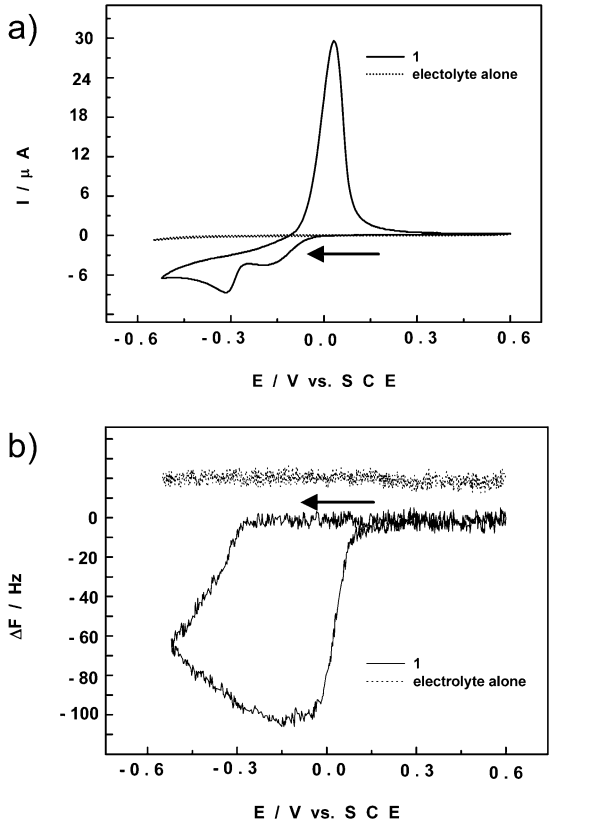

Figure 6. (a) Cyclic voltammogram of a 10^{-4} M solution of **1** in a pH 5 medium, restricted to the copper waves and run on the carbon film of the EQCM crystal. The cyclic voltammogram of the pure pH 5 medium is superimposed for comparison. The scan rate was 10 mV s^{-1}. (b) EQCM frequency responses run simultaneously with both cyclic voltammograms in Figure 6a.

+0.2 to −0.520 V, the mass increase (alternatively the frequency decrease) is seen to start at ∼ −0.28 V, a potential at which the reduction of Cu(I) to Cu(0) can be considered to start. This observation indicates that, in the potential domain of the Cu(II) to Cu(I) process, no deposition of Cu(0) occurs, as the frequency variation recorded in this domain is comparable to the one recorded in the electrolyte alone (Figure 6b). The CVs recorded as a function of the potential scan rate between 2 and 100 mV s^{-1} do not show any significant deposition of Cu(0). To our knowledge, this is the first time that EQCM has been used to demonstrate the stabilization of a Cu(I) state by a POM ligand. During the reverse potential scan (from −0.520 to +0.2 V), a weak deposition continues, as a consequence of the competition between the oxidation of Cu(0) and the two-electron reduction of Cu(II) to Cu(0) (from −0.520 to −0.03 V). Finally, the mass decrease starts only at −0.03 V, i.e., after the beginning of the oxidation of Cu(0) at −0.110 V. It must be noted that a CV alone cannot be used to determine this inception potential for Cu(0) oxidative desorption. Upon complete reoxidation of Cu(0), it is remarkable that the electrode recovers the initial mass it had before the copper deposition, which is not always the case, depending on the Cu-substituted POM used to perform the deposition.[31] From

(31) Keita, B.; Abdeljalil, E.; Nadjo, L.; Contant, R.; Belghiche, R. *Langmuir* **2006**, *22*, 10416.

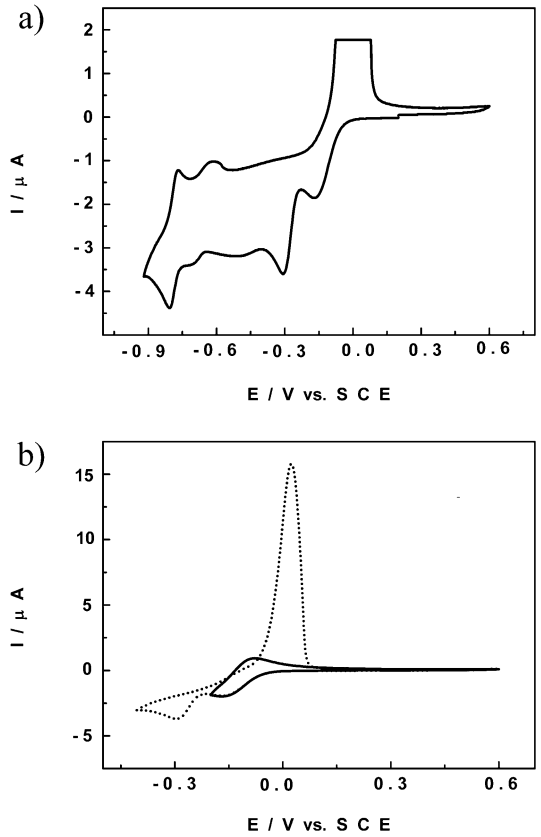

Figure 7. (a) Cyclic voltammograms of 4.8×10^{-5} M solutions of **2** in a pH 5 medium highlighting the presence a drawn-out and irreversible wave, extending roughly from −0.400 to −0.650 V. The copper reoxidation wave was truncated. The scan rate was 10 mV s^{-1}, the working electrode was glassy carbon (3 mm diameter disc), and the reference electrode was SCE. The same experimental conditions are valid for Figure 7b, unless otherwise stated. (b) Cyclic voltammograms of **2** restricted to the potential domain of copper waves: the potential reversal is fixed respectively after the Cu(II) to Cu(I) redox process and after the Cu(I) to Cu(0) process.

a practical point of view, this result is worth stressing for analytical applications using Cu(0) films deposited in situ. As a matter of fact, it is very useful to deposit films that could be easily removed by electrochemical oxidation, thus regenerating the electrode surface.[32]

Supporting Information Figure SI5 displays all the chemically reversible waves of **2** at pH 5. This CV is constituted by two close reduction waves well-separated from another group of two closely spaced waves. Upon magnification of the CV, a drawn-out and irreversible wave was observed (Figure 7a), extending roughly from −0.400 to −0.650 V, the aforementioned four reduction waves peaking respectively at −0.164, −0.306, −0.716, and −0.806 V. The characteristics of the two last waves are close to those of the POM precursor.[30c] The characteristics of the first two waves are close to those described previously for the reduction of the Cu(II) centers of **1**. To find out the process occurring on the drawn-out irreversible wave, a controlled-potential coulometry was performed on this wave. As a result, the characteristic Cu(0) deposition on the working electrode surface was observed and the solution did not turn blue, a feature that would have revealed a reduction of W centers. It comes out that this third wave must also be attributed to the reduction of the Cu(II) centers. Such an observation is not surprising, because all the Cu(II) centers of **2** are not strictly equivalent, a structural feature that opens the possibility for several separated reduction steps for these centers, as already found with other sandwich-type POMs.[30b,33] It must be noted that the extent of separation of these waves depends on the pH of the medium, the waves getting closer when the pH was decreased. In any case, exactly as observed with **1**, the first reversible reduction wave of **2** features the reduction of Cu(II) to Cu(I), as appearing in Figure 7b. In addition, in the electrolyte used, the Cu(II) centers remain stable within polyanion **2**: as a matter of fact, comparison of the peak current intensities for the Cu(II) to Cu(I) reduction processes for **2** and for $Cu(SO_4)$, at the same concentration, indicates the diffusion coefficient of **2** to be roughly 8 times smaller than that for $Cu(SO_4)$, thus demonstrating that the Cu(II) cations remain within the complex in solution. Interesting observations were made during controlled-potential electrolyses that aimed at elucidating the processes occurring on each wave: (i) When the fixed potential is less negative than −0.6 V, the only observed process is the Cu(0) deposition; however, with a critical choice of the electrolysis potential to avoid even the slightest reduction of W centers, coulometry gives a consumption of (39.8 ± 0.4) electrons per molecule of **2**, thus indicating that all copper centers are two-electron reduced. (ii) As soon as the potential is more negative than −0.6 V, a strong catalysis of the solvent reduction is observed; this catalysis is so important that the amount of reduced W centers, as judged from the associated characteristic blue color, is very weak, even after the consumption of several times the charge necessary to reduce all the W centers. It is worth noting that the catalysis is much stronger than that observed with the lacunary POM precursor.

Electrocatalysis of Dioxygen Reduction. The reversibility of the Cu(II)/Cu(I) process within polyanions **1** and **2** associated with their accumulation in these complexes, resulting in multiplication of this one-electron process, opens the way for electrocatalytic reactions usually triggered by this redox system. Also, the efficiency of POMs in the catalytic or electrocatalytic reduction of dioxygen has been known for a long time,[34] but most of the unsubstituted POM-based catalysts are efficient in relatively acidic media (pH ≤ 4), with overpotentials that remain important. Recently, it was demonstrated that Cu(II)-substituted POMs, α_2-$[Cu(OH_2)P_2W_{15}Mo_2O_{61}]^{8-}$ [31,35] and $[Cu_4(H_2O)_2(P_2W_{15}O_{56})_2]^{16-}$ [30b] are efficient in the electrocatalytic reduction of dioxygen in the 2−5 pH range. We have then studied the efficiencies of compounds **1** and **2** for the electrocatalytic reduction of dioxygen.

Figure 8a shows the CV pattern of polyanion **1** restricted to the Cu(II)/Cu(I) redox couple in the absence and presence

(32) Welch, C. M.; Hyde, M. E.; Banks, C. E.; Compton, R. G. *Anal. Sci.* **2005**, *21*, 1421.

(33) Mbomekalle, I. M.; Keita, B.; Nadjo, L.; Berthet, P.; Hardcastle, K. I.; Hill, C. L.; Anderson, T. M. *Inorg. Chem.* **2003**, *42*, 1163.

(34) (a) Keita, B.; Nadjo, L.; Haeussler, J. P. *J. Electroanal. Chem.* **1988**, *243*, 481. (b) Papaconstantinou, E. *J. Chem. Soc., Chem. Commun.* **1982**, 12, and references therein.

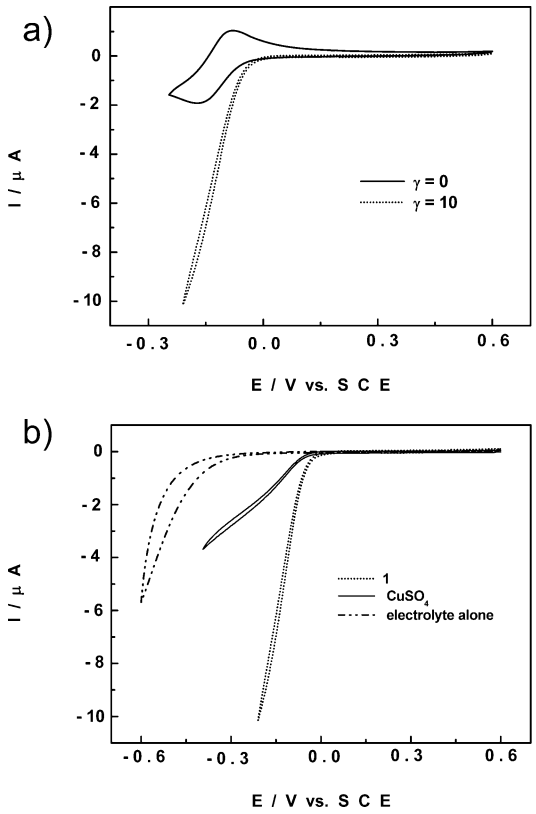

Figure 8. (a) CV pattern of polyanion **1** restricted to the Cu(II)/Cu(I) redox couple in the absence and presence of dioxygen in a pH 5 medium. The excess parameter γ is defined as: $\gamma = [O_2]/[\mathbf{1}]$ The scan rate was 10 mV s^{-1}, the working electrode was glassy carbon (3 mm diameter disc), and the reference electrode was SCE. (b) Comparison of the CV patterns corresponding to the reduction of dioxygen in the absence of any catalyst (electrolyte alone), in the presence of a 10^{-4} M solution of $Cu(SO_4)$, or in the presence of a 10^{-4} M solution of **1**. The excess parameter γ is defined as $\gamma = [O_2]/[Cu(SO_4)]$ or [**1**], and its value was $\gamma = 10$. The scan rate was 10 mV s^{-1}, the working electrode was glassy carbon (3 mm diameter disc), and the reference electrode was SCE.

of dioxygen at pH 5 at a scan rate of 10 mV s^{-1}. With dioxygen, an important increase of the cathodic wave is observed in the potential domain of the Cu(II)/Cu(I) process. Concomitantly, the chemical reversibility of this last process is suppressed. In addition, the CV recorded in this potential domain between 2 and 200 mV s^{-1} indicates the catalysis to be fast enough to maintain the irreversibility of the catalytic wave whatever the potential scan rate. Figure 8b compares the CVs corresponding to the direct reduction of dioxygen on the glassy-carbon electrode, in the presence of $Cu(SO_4)$, and in the presence of **1**. Obviously, the presence of **1** facilitates the reduction of dioxygen by showing both the largest decrease in overpotential and the best overall kinetics of the CV as shown in Figure 8b. These observations demonstrate the efficient catalysis of dioxygen reduction during the Cu(II) to Cu(I) reduction process in **1**. When the catalytic current contains a component due to the reduction of the POM itself, the catalytic efficiency can be defined as $CAT = 100 \times [I(POM + O_2) - I(POM)]/I(POM)$, where $I(POM)$ is the current for the reduction of the POM in the absence of O_2 and $I(POM + O_2)$ is the value of the current observed in the presence of O_2. First, we have checked that the CAT values increase with increasing γ parameter, which indicates the effective reduction of dioxygen. Second, calculated CAT values at pH 5, in identical experimental conditions, indicate that **1** shows a distinctly larger catalytic efficiency than other Cu-containing sandwich-type POMs like $[Cu_4(H_2O)_2(X_2W_{15}O_{56})_2]^{16-}$ ($Cu_4X_4W_{30}$) (X = P, As).[30b] For example, at pH 5, in the same experimental conditions, polyanion **1** is roughly 4.6 times more efficient than $Cu_4P_4W_{30}$. This large difference in CAT values should probably be traced mainly to the important difference in the potential locations of the Cu(II) to Cu(I) processes in the two POMs: actually, this process appears at a potential 0.324 V more positive for **1** than for $Cu_4P_4W_{30}$.

With the characteristics of the Cu(II)/Cu(I) couple comparable to those observed for this couple in **1**, polyanion **2** also shows an important electrocatalytic activity in the reduction of dioxygen, which is roughly 5.7 times more important than that of $Cu_4P_4W_{30}$. Finally, it must be noted that **2** is slightly more efficient than **1**.

One of the important aspects of the reduction of dioxygen is the nature of the final product. In acid media, two-electron reduction yields hydrogen peroxide; the four-electron product is water, which can be obtained either directly or through the intermediate formation of hydrogen peroxide that is further reduced.

In the present work, polyanions **1** and **2** are found to reduce H_2O_2 in the same potential domain as O_2, H_2O_2 being slightly easier to reduce at pH 5. Therefore, on considering the relative potential locations of the reduction waves, water is expected to be the final product of dioxygen reduction. With the aim to check the effectiveness of this conclusion, large-scale electrolyses of **1** in the presence of dioxygen were performed, with the potential set at −0.150 V. Typically, in one of the several replications of this electrolysis, 220 electrons per polyanion **1** molecule were consumed, which should have generated 1.1×10^{-2} M H_2O_2 if this species was the final product. At the end of each electrolysis, the amount of generated H_2O_2 was tested by spectrophotometry, using, as reagent, the sensitive $Ti(SO_4)_2$.[36] Whatever the batch, only traces of H_2O_2 were detected. This observation indicates that the final oxygen-containing product is essentially water. The presence of transient H_2O_2 can be suspected, as traces of this chemical were detected. This result is in agreement with the previous observation that polyanions **1** and **2** reduce H_2O_2 and O_2 in the same potential domain.

Finally, it can be concluded that the electrocatalytic reduction of dioxygen by **1** and **2** is an overall four-electron process giving water.

Conclusions

We have shown here that two-dimensional and high-nuclearity molecular POM azido compounds can be isolated. While the synthesis of these species has been performed in the presence of a large excess of N_3^-, single X-ray diffraction

(35) Keita, B.; Benaissa, M.; Nadjo, L.; Contant, R. *Electrochem. Commun.* **2002**, *4*, 663.
(36) Vogel, A. I. *Quantitative Inorganic Analysis*; Longmans: London, 1960.

data revealed that the paramagnetic centers are connected via both azido and hydroxo ligands, as previously observed for the tetranuclear complex $[(A\text{-}\alpha\text{-}SiW_9O_{34})Co_4(OH)(\mu_{1,1,1}\text{-}N_3)_2(CH_3COO)_3]^{8-}$.[10] It then appears that the synthesis of POMs containing 3d cations only bridged by azido groups is difficult when polylacunary POM ligands possessing more than two vacancies are used as precursors. The magnetic behavior of both compounds is dominated by antiferromagnetic interactions. Electrochemical measurements together with electronic absorption spectroscopy and gel filtration chromatography revealed that **1** and **2** are stable in aqueous solution at pH 5. Additionally, for both compounds, the stability of the Cu(II)/Cu(I) couple is remarkable compared with the observations made in other Cu(II)-substituted POMs. Moreover, EQCM measurements have demonstrated that in solution the formation of the Cu(I) species can occur without the formation of Cu(0). It can then be proposed that such POMs incorporating Cu(I) cations could be isolated. The electrocatalytic reduction of dioxygen and hydrogen peroxide was achieved efficiently. The dioxygen reduction is an overall four-electron process with water as the final product, and only traces of hydrogen peroxide have been detected even when large-scale electrolyses of **1** in the presence of dioxygen were performed. Noticeably, the beneficial effect of the accumulation of 3d transition-metal centers in the POM matrix on the electrocatalytic process has been evidenced.

Acknowledgment. This work was supported by the CNRS (UMR 8000, 8180, and 8613), the University of Paris-Sud, and the University of Versailles Saint-Quentin. The help of Dr P. de Oliveira with one of the stability experiments is acknowledged.

Supporting Information Available: X-ray crystallographic files in CIF format for **1** and **2**; UV−vis spectra of compounds **1** (Figure SI1a) and **2** (Figure SI1b) in aqueous solution; $\chi_M T = f(T)$ curve relative to compound **2** (Figure SI2); cyclic voltammograms of **1** restricted to the potential domain of the Cu(II) to Cu(I) redox process (Figures SI3 and SI4); cyclic voltammogram of **2** (Figure SI5). This material is available free of charge via the Internet at http://pubs.acs.org.

IC070313W